

Optically active Er³⁺ ions in SiO₂ codoped with Si nanoclusters

D. Navarro-Urrios,^{1,a)} Y. Lebour,¹ O. Jambois,¹ B. Garrido,¹ A. Pitanti,² N. Daldosso,² L. Pavesi,² J. Cardin,³ K. Hijazi,³ L. Khomenkova,³ F. Gourbilleau,³ and R. Rizk³
¹MIND-IN2UB, Dept. Electrònica, Universitat de Barcelona, Martí i Franquès 1, 08028 Barcelona, CAT, Spain
²Dipartimento di Fisica, Laboratorio di Nanoscienze, Università di Trento, Via Sommarive 14, I-38100 Povo (Trento), Italy
³CIMAP, UMR CEA/CNRS 6252, 6 Boulevard Maréchal Juin, 14050 CAEN Cedex 4, France

(Received 27 May 2009; accepted 29 September 2009; published online 6 November 2009)

Optical properties of directly excited erbium (Er³⁺) ions have been studied in silicon rich silicon oxide materials codoped with Er³⁺. The spectral dependence of the direct excitation cross section (σ_{dir}) of the Er³⁺ atomic $^4I_{15/2} \rightarrow ^4I_{11/2}$ transition (around 0.98 μm) has been measured by time resolved μ -photoluminescence measurements. We have determined that σ_{dir} is $9.0 \pm 1.5 \times 10^{-21} \text{ cm}^2$ at 983 nm, at least twice larger than the value determined on a stoichiometric SiO₂ matrix. This result, in combination with a measurement of the population of excited Er³⁺ as a function of the pumping flux, has allowed quantifying accurately the amount of optically active Er³⁺. This concentration is, in the best of the cases, 26% of the total Er population measured by secondary ion mass spectrometry, which means that only this percentage could provide optical gain in an eventual optical amplifier based on this material. © 2009 American Institute of Physics. [doi:10.1063/1.3253753]

I. INTRODUCTION

Er doped materials have been subject of an extensive research on the last decades, principally since they are used as the active media for fiber optical amplifiers and lasers operating at 1.55 μm in long-haul communications technology. In planar optical amplifiers or lasers integrated in photonic circuits, where small overall sizes are required, the presence of Er³⁺ sensitizers allows achieving high degrees of population inversion for low pumping fluxes even if reasonably high Er³⁺ concentrations are present.¹ During the last years, Si nanoclusters (Si-nc) embedded in a SiO₂ matrix have become one of the most promising Er³⁺ sensitizers. In fact, the presence of Si-nc significantly enhances and broadens in energy the effective excitation cross section (σ_{eff}) of the Er³⁺ ions as a result of an efficient energy transfer mechanism.^{2,3} The restrictive conditions to be fulfilled for a pumping source could be thus relaxed, and either electrical⁴ or low-power broadband light sources⁵ would be possible. In addition, this composite material is fabricated using standard silicon complementary metal-oxide semiconductor processes. Great efforts have been dedicated by a broad scientific community during the last years toward understanding the physics of the system and overcoming the small percentages of the total Er population that can take advantage of the indirect excitation mechanism.⁶⁻⁹ However, the complete understanding of the indirect excitation mechanism is still under debate. Recently, even the role of the Si-nc in the indirect transfer has been questioned¹⁰ and it has been postulated that luminescent centers could play the main sensitization role instead of the Si-nc. In any case, although it seems clear that the low percentages are mainly related with the short range

interaction distance of the energy transfer process and could be progressively improved,¹¹ it has been additionally proposed that up to several tens percent of the remaining Er content could not be even optically active,^{6,12} i.e., not able to emit light even if pumped directly. In samples with a significant Er³⁺ coupled content, the inactive population starts to be a pressing issue to address a further optimization of the material. Hence, it turns essential to study the optical properties of the optically active Er³⁺ content and quantify accurately its concentration (N_{Er}), which is proportional to the maximum potential internal gain that the material would provide. The coupled Er³⁺ content should be thus compared to N_{Er} and not to the total content.

In this work we have assessed N_{Er} in samples with high coupled Er³⁺ content by performing quantitative measurements of the Er³⁺ population found in the $^4I_{13/2}$ state (N_2) as a function of the photon flux (Φ) when pumping the ions at 0.98 μm (resonant to the direct $^4I_{15/2} \rightarrow ^4I_{11/2}$ transition). Such a pumping wavelength only allows direct excitation of Er³⁺ ions, since exciton formation within the Si-nc is very improbable. This is a key point of the present work because it both prevents indirect excitation and ensures no energetic exchange from directly excited Er³⁺ to the Si-nc. In fact, when pumping resonantly with Er³⁺ transitions at wavelengths in the UV-visible region, excitons are created within the Si-nc. Under these pumping conditions, it has been postulated the possibility that excited ions relax nonradiatively by transferring the energy to the confined carriers, producing an allowed carrier excitation among intraband levels.⁹ This effect would not distinguish if the excitation has been done by direct or indirect excitation and would reduce the excited state population with respect to a case where no excitons are present.

^{a)}Electronic mail: dnavarro@el.ub.es.

The saturation value of N_2 gives the total erbium content that can actually be inverted, i.e., N_{Er} , among the total one,

$$N_2 = \frac{\sigma_{\text{dir}} N_{\text{Er}} \Phi}{\sigma_{\text{dir}} \Phi + 1/\tau_d}, \quad (1)$$

where τ_d is the total decay lifetime of the transition and σ_{dir} is the direct excitation cross section at 0.98 μm . It is worth to note that if the pumping flux is low enough to neglect the product $\sigma_{\text{dir}} \Phi$ with respect to the inverse of τ_d a linear approximation with Φ of Eq. (1) is valid ($N_2 \approx \sigma_{\text{dir}} \tau_d N_{\text{Er}} \Phi$). In any case, in order to apply Eq. (1) accurately, the exact values of τ_d and σ_{dir} should be determined independently for each sample under study. However, the direct quantification of σ_{dir} for these purposes is generally skipped and its value is assumed to be that of Er in a stoichiometric SiO_2 matrix, giving rise to an important uncertainty in the N_{Er} extracted values.^{12,13} The main reason for the lack of σ_{dir} values in the UV-visible region is the mentioned enhancement of σ_{eff} , which, in addition, is a magnitude that depends on the distance of the particular ion with respect to the Si-nc surface.⁸ In the spectral region of the ${}^4I_{15/2} \rightarrow {}^4I_{13/2}$, ${}^4I_{11/2}$ transitions, the accurate determination of σ_{dir} is also not straightforward. In fact, with the absorption techniques used in Refs. 13 and 14, it is only possible to extract the optical losses of the material that are given by the product $\sigma_{\text{dir}} N_{\text{Er}}^{\text{ab}}$ where $N_{\text{Er}}^{\text{ab}}$ is the Er^{3+} content able to absorb light. $N_{\text{Er}}^{\text{ab}}$ is an unknown quantity that could be lower than the total content and greater than N_{Er} . In this work we present a different approach based on time resolved μ -photoluminescence (μ -PL) measurements that has allowed the first direct assessment of the spectral dependence of σ_{dir} around 0.98 μm for this material.

II. EXPERIMENTAL DETAILS

Two layers have been fabricated with the magnetron sputtering technique. Sample A was grown at 500 $^\circ\text{C}$ under argon pressure by the cosputtering of three targets (SiO_2 , Er_2O_3 , and Si),¹⁵ while sample B was deposited at 100 $^\circ\text{C}$ under argon-hydrogen mixture by the cosputtering of pure SiO_2 and Er_2O_3 targets.¹⁶ These samples are the result of an optimization process until achieving maximum PL signal and total lifetime under 476 nm excitation, which is not resonant with an Er^{3+} direct transition. The compositions of the samples were measured x-ray photoelectron spectroscopy and secondary ions mass spectroscopy: 8.5 at. % of Si excess and 3.6×10^{20} Er/cm^3 for sample A and 5 at. % of Si excess and 3.4×10^{20} Er/cm^3 for sample B.¹⁶ Both layers were annealed at 910 $^\circ\text{C}$ during 60 min in pure nitrogen flow and have a refractive index of about 1.51 at 1.55 μm , while the thicknesses were 1.36 and 1.22 μm for samples A and B, respectively. In particular, in sample B it was determined an absolute Er^{3+} concentration efficiently coupled to the Si-nc of 3.6×10^{19} cm^{-3} , i.e., 11% of the total Er content.¹⁷ A soda-lime 1.3 mm thick sample supplied by Corning, doped with Er to a density of 0.7×10^{20} at/cm^3 , was used as a reference.

Quantitative continuous wave PL experiments were performed by pumping with a 975 nm semiconductor laser

(~ 0.2 W maximum power) focused with a 15 cm focal length lens onto a surface of 5×10^{-4} cm^2 over the samples, which allowed achieving pumping photon fluxes (Φ) as high as 10^{21} ph/cm^2 s. Since the depth of focus of the lens is much longer than the studied samples thicknesses, the pump spot surface can be assumed as constant along them. The PL emission was analyzed with a monochromator and detected with an InGaAs photomultiplier tube. The quantification of N_2 was accomplished by calibrating our detection system with the reference sample, in which the Er^{3+} concentration is fully active and whose cross sections and radiative and total lifetimes are known. The theoretical photon flux emitted (Φ_{em}) by this sample at a certain pumping photon flux is calculated and used to calibrate the detection system. After this calibration procedure, the emitted flux from any sample can be directly calculated from a PL measurement.

N_2 can be related with Φ_{em} in the following way:

$$N_2 = \frac{\Phi_{\text{em}} \tau_{\text{rad}}}{V}, \quad (2)$$

where V is the pumped volume. The radiative lifetime (τ_{rad}) was estimated to be 16 ms in the studied samples taking into account the change in the refractive index with respect to the pure SiO_2 case ($\tau_{\text{rad}} = 18$ ms) in accordance with Ref. 18.

For determining σ_{dir} we have done time resolved μ -PL measurements, where the pump laser has been modulated externally. The rise and decay lifetimes (τ_r , τ_d) of the 1.55 μm PL signal were determined as a function of Φ in a high Φ regime ($\Phi > 10^{22}$ ph/cm^2 s). For a quasitwo level system under these experimental conditions it is possible to demonstrate that⁸

$$\frac{1}{\tau_r} - \frac{1}{\tau_d} = \sigma_{\text{dir}} \Phi. \quad (3)$$

It is worth noting that, since the expected cross section is very low ($\sim 10^{-21}$ cm^2) very high fluxes are required to observe non-negligible differences between the rise and decay lifetimes.

The setup scheme used for performing these measurements is shown in Fig. 1(c). The laser beam was passed through a beam splitter while a charge-coupled-device (CCD) camera was placed on the remaining free optical line. For achieving the required high Φ it was focused into a micrometric spot (3×10^{-7} cm^2 area) by a microscope objective. It is worth noting that the spot surface is more than three orders of magnitude smaller than in the case of the standard PL measurements reported before. The CCD camera allows observing the dimensions of the pumping spot on the sample when the latter is on the focus of the objective. Figure 1(b) shows the real image of the laser spot on the top of a reference structure that is 32 μm wide. This setup has been also used for performing PL measurements at high Φ .

III. EXPERIMENTAL RESULTS AND DISCUSSION

In Fig. 1(a) we show the actual time-resolved (TR)-PL measurement. The 1.55 μm PL signal temporal behavior of sample A when the pump is switched on (rise) and off (decay) is presented. The rise PL signals have been measured

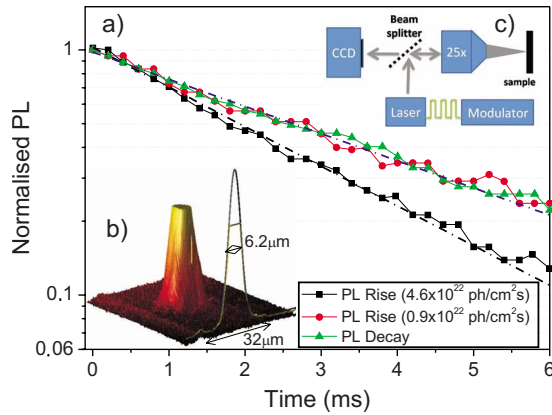


FIG. 1. (Color online) (a) Experimental PL rise for high (squares) and low (circles) Φ inverted and normalized for clarity, and PL decay (triangles). The dashed lines are the single exponential fits of the experimental data. (b) Analysis of the spatial energy distribution of the pumping spot on the surface of a 32 μm waveguide. (c) Scheme of the experimental setup built for the μ -PL time resolved experiments.

for minimum (circles) and maximum (squares) photon flux. The lifetime of the rising signal noticeably increases by lowering Φ , converging to the PL decay lifetime (triangles) at low Φ . All the set of decaying and rising signals fit very well to a single exponential law (dashed-dotted lines), thus allowing the determination of τ_r and τ_d . The decay lifetimes were determined to be 4.2 ms for sample A and 4.8 ms for sample B independently of Φ .

In the inset of Fig. 2 we represent the left part of Eq. (3) as a function of Φ for both samples. The slope of the linear fit, which has been forced to pass by zero, gives $\sigma_{\text{dir}}(975 \text{ nm}) = 3.1 \pm 0.5 \times 10^{-21} \text{ cm}^2$, which is roughly the same for the two samples under study.

The PL signal corresponding to the ${}^4I_{11/2} \rightarrow {}^4I_{15/2}$ transition observed in those samples (Fig. 2, dashed curve) is, in a first approximation, proportional to the emission cross section σ_{em} . Thus, it is possible to relate the latter with σ_{dir} by using McCumber theory,¹⁹ which results in

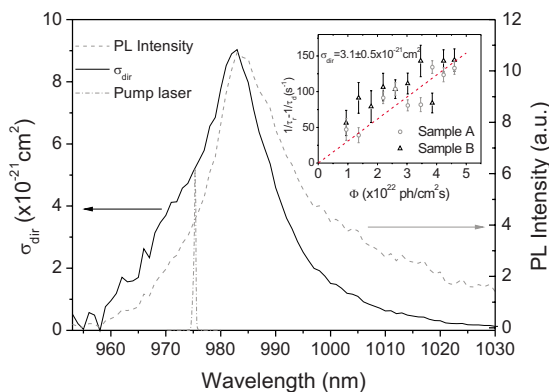


FIG. 2. (Color online) PL emission (dashed line) corresponding to the ${}^4I_{11/2} \rightarrow {}^4I_{15/2}$ transition. It has been obtained by pumping at low Φ at 488 nm. The solid curve shows the extracted spectrum for the excitation cross section of the ${}^4I_{15/2} \rightarrow {}^4I_{11/2}$ transition. The dashed-dotted gray curve shows the spectrum of the pump laser used in the present study. (Inset panel) Difference of the inverses of the rise and decay lifetimes as a function of Φ for samples A (gray circles) and B (black triangles). The dashed curve corresponds to the fit using Eq. (2).

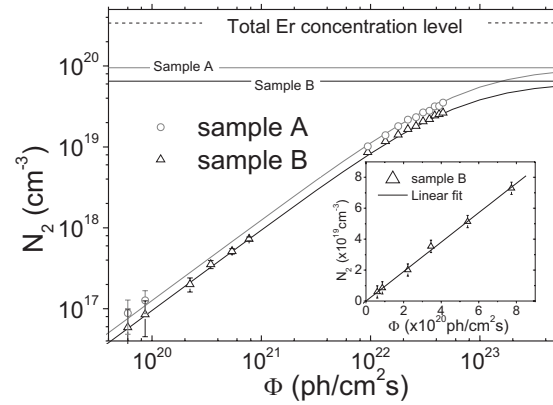


FIG. 3. N_2 as a function of Φ (in log-log scale) for samples A (gray circles) and B (black triangles) together with their respective fits using Eq. (1). The different achievable concentration levels are also represented as horizontal lines. The inset represents the low Φ set of data for sample B in a linear scale together with a linear fit using the low flux approximation of Eq. (1).

$$\sigma_{\text{dir}}(\lambda) = \sigma_{\text{em}}(\lambda) \exp \left[\frac{hc}{kT} (1/\lambda - 1/\lambda_m) \right], \quad (4)$$

where λ_m is defined as the wavelength of the transition between the lowest levels of the two manifolds involved. We have applied Eq. (4) to the PL spectrum to extract the spectral shape of σ_{dir} and then normalized the resulting curve by using the measured value at 975 nm in order to have the actual values. The result is the spectral dependence of the σ_{dir} for the ${}^4I_{15/2} \rightarrow {}^4I_{11/2}$ transition (Fig. 2, solid curve, left axis).

At the maximum of the transition the extracted σ_{dir} is $9.0 \pm 1.5 \times 10^{-21} \text{ cm}^2$, whereas the values found in the literature for Er^{3+} doped silicate glasses without Si excess are all about $2\text{--}5 \times 10^{-21} \text{ cm}^2$ at the peak wavelength.²⁰ The observed twofold enhancement in the material under study is associated to differences in the effective crystal field potential at the ion site,²⁰ since the refractive index difference with respect to the silicate cases is too small (less than 3%) to have a significant effect. This small enhancement is quite consistent with the one recently reported for the ${}^4I_{15/2} \rightarrow {}^4I_{13/2}$ transition,^{13,14} although the determination of those values have the limitations described previously.

In Fig. 3 we show the quantitative determination of N_2 for both samples as a function of Φ . Two ranges of Φ are reported: low Φ ($10^{20}\text{--}10^{21} \text{ ph/cm}^2 \text{ s}$) obtained with the standard PL setup (calibrated as described previously) and high Φ ($10^{22}\text{--}10^{23} \text{ ph/cm}^2 \text{ s}$) obtained with the μ -PL setup. Since the linear approximation of Eq. (1) is valid in the low Φ range and τ_d and σ_{dir} are already known, it is possible to extract N_{Er} from the slope of the linear fit. This is reported in the inset of Fig. 3 for the case of sample B and the extracted value is $N_{\text{Er}} = 0.64 \times 10^{20} \text{ cm}^{-3}$, which is only 19% of the total Er^{3+} content present in this sample ($3.4 \times 10^{20} \text{ cm}^{-3}$).

The PL data obtained at high Φ showed for both samples a sublinear behavior, which indicates that the linear approximation made for low fluxes is no longer valid and the saturation of N_2 is starting to be achieved. In order to extract the quantitative data of N_2 at high Φ it is not possible to use the reference sample for calibrating the μ -PL setup since the

depth of focus of the objective (tens of micrometers) is significantly smaller than the reference sample thickness (1.3 mm). This makes Φ vary significantly along this sample as the beam spot changes its surface so that the determination of Φ_{em} requires the resolution of a complex integral. This is not an issue on samples A and B since the thickness of the active layer is small enough with respect to the depth of focus, so Φ (and, thus, N_2) can be considered constant.

Therefore, in order to determine the total flux emitted by a sample (and thus extract N_2 from the high Φ PL signals taken) we have used the N_2 data taken at low Φ for sample B and then normalized the high Φ data by a factor that optimizes the fitting using Eq. (1) (after introducing the measured values of τ_d and σ_{dir}). This procedure has allowed us to extract a value of $N_{\text{Er}} = 0.64 \times 10^{20} \text{ cm}^{-3}$ for sample B, which is the very same value obtained by using only the points at low Φ , demonstrating the reliability of the followed procedure for calibrating the μ -PL setup.

The high flux N_2 data of sample A have been represented together with the low flux data and fitted afterwards using Eq. (1). A further demonstration of the accurate calibration of the μ -PL setup is that the fitted curve reproduces quite well both set of data obtained with different setups.

Although it has already been stated that σ_{dir} and the total Er^{3+} content are roughly the same for both samples, N_2 is visibly higher for sample A. Indeed, for sample A we have obtained $N_{\text{Er}} = 0.97 \times 10^{20} \text{ cm}^{-3}$ (26% of the total Er^{3+} content, i.e., $3.6 \times 10^{20} \text{ cm}^{-3}$), slightly greater than what is obtained for sample B. These values are compatible with those reported for example in Ref. 6, although in that case the data were extracted by pumping in the visible and assuming a direct cross section equal to that of Er^{3+} in stoichiometric SiO_2 .

With the determined values for N_{Er} the potential gain in an amplifier will be reduced by at least a factor of 3 with respect to what would be given by the total Er^{3+} content. For sample B, this quantity can be compared with the indirectly excitable concentration that is able to emit light, revealing that about 53% of the optically active content (11% of the total content) is coupled to the Si-nc and thus invertible by indirect excitation. This means that in principle it is possible to invert the population of optically active Er^{3+} by exploiting the indirect excitation of Si-nc.

If the remaining erbium content that is not emitting light is either (i) totally inactive or (ii) unable to efficiently emit light (although being able to absorb it) remains an open issue out of the scope of this paper. Further spectral quantitative measurements of the direct absorption coefficient would be required for determining the Er^{3+} concentration able to absorb light, which is not possible to be extracted from PL measurements. In our opinion hypothesis (ii) is more reasonable since various possible configurations of Er^{3+} within the matrix could efficiently quench the radiative recombination paths. At this stage, we can only speculate that, since experimentally the PL single exponential decays are independent on Φ with a quite long lifetime the emitting Er^{3+} population does not suffer from strong cooperative up-conversion mechanisms (otherwise the PL lifetime would be reduced as a function of Φ as the initial value of N_2 becomes higher).¹⁷

Therefore, the hypothesis (ii) would imply the existence of two completely different kinds of Er^{3+} ions populations: one able to recombine radiatively with roughly the same probability and another surrounded by quenching centers where the radiative recombination probability is negligible with respect to the nonradiative one. A compatible scenario with the previous statement would be that the nonemitting Er^{3+} population is placed within the Si-nc or that it suffers from local concentration quenching effects (in a way that the excitation can migrate from one ion to another until it encounters a quenching center where a local phonon or deformation can deactivate the excitation). Indeed, it has already been reported in bulk glass that the local structure of the material can vary, such that clusters of ions can form in one region whereas another region might have isolated ions.^{21,22} A similar observation has been reported for ion implanted Si rich SiO_2 codoped with Er^{3+} , which could contribute to the low percentages of indirectly excitable Er^{3+} content reported.²³ It is possible that further annealing would improve the optically active Er^{3+} content as reported for example in Ref. 24 in Er^{3+} doped stoichiometric SiO_2 samples. However, following this procedure, we have observed a decreasing in the Er^{3+} content that can be excited indirectly.²⁵

IV. CONCLUSIONS

In conclusion, we have made a novel study on the optical properties of the directly excited Er^{3+} ions in an Er^{3+} doped SiO_2 sensitized by Si nanoclusters material, quantifying both the spectral dependence of the direct excitation cross section of the ${}^4I_{15/2} \rightarrow {}^4I_{11/2}$ transition and the optically active Er^{3+} concentration. We have observed a twofold enhancement of the direct cross section with respect to the values reported in the literature for silicate glasses. On the other hand, it has been demonstrated that, in the best of the studied samples, 26% of the total Er^{3+} concentration is able to emit light at $1.55 \mu\text{m}$ when directly excited, result that may impact in the potential performances of this material for amplification purposes.

ACKNOWLEDGMENTS

The authors thank the financial support by EC through the LANCER Project (Grant No. FP6-IST 033574) and kindly acknowledge Dr. C. J. Oton for fruitful discussions. One of the authors thanks the Spanish Ministry of Education and Science through the Juan de la Cierva program.

¹A. Polman and F. C. J. M. van Veggel, *J. Opt. Soc. Am. B* **21**, 871 (2004).

²A. J. Kenyon, P. F. Trwoga, M. Federighi, and C. W. Pitt, *J. Phys.: Condens. Matter* **6**, L319 (1994).

³F. Priolo, G. Franzò, D. Pacifici, V. Vinciguerra, F. Iacona, and A. Irrera, *J. Appl. Phys.* **89**, 264 (2001).

⁴F. Iacona, D. Pacifici, A. Irrera, M. Miritello, G. Franzò, and F. Priolo, *Appl. Phys. Lett.* **81**, 3242 (2002).

⁵J. Lee, J. H. Shin, and N. Park, *J. Lightwave Technol.* **23**, 19 (2005).

⁶M. Wojdak, M. Klik, M. Forcales, O. B. Gusev, T. Gregorkiewicz, D. Pacifici, G. Franzò, F. Priolo, and F. Iacona, *Phys. Rev. B* **69**, 233315 (2004).

⁷P. G. Kik and A. Polman, *J. Appl. Phys.* **88**, 1992 (2000).

⁸B. Garrido, C. García, S.-Y. Seo, P. Pellegrino, D. Navarro-Urrios, N. Daldosso, L. Pavesi, F. Gourbilleau, and R. Rizk, *Phys. Rev. B* **76**, 245308 (2007).

- ⁹I. Izeddin, A. S. Moskalenko, I. N. Yassievich, M. Fujii, and T. Gregorkiewicz, *Phys. Rev. Lett.* **97**, 207401 (2006).
- ¹⁰O. Savchyn, F. R. Ruhge, P. G. Kik, R. M. Todi, K. R. Coffey, H. Nukala, and H. Heinrich, *Phys. Rev. B* **76**, 195419 (2007).
- ¹¹D. Navarro-Urrios, A. Pitanti, N. Daldosso, F. Gourbilleau, R. Rizk, B. Garrido, and L. Pavesi, *Phys. Rev. B* **79**, 193312 (2009).
- ¹²S. Minissale, T. Gregorkiewicz, M. Forcales, and R. G. Elliman, *Appl. Phys. Lett.* **89**, 171908 (2006).
- ¹³N. Daldosso, D. Navarro-Urrios, M. Melchiorri, L. Pavesi, C. Sada, F. Gourbilleau, and R. Rizk, *Appl. Phys. Lett.* **88**, 161901 (2006).
- ¹⁴H. Mertens, A. Polman, I. M. P. Aarts, W. M. M. Kessels, and M. C. M. van de Sanden, *Appl. Phys. Lett.* **86**, 241109 (2005).
- ¹⁵K. Hijazi, L. Khomenkova, J. Cardin, F. Gourbilleau, and R. Rizk, *Physica E* **41**, 1067 (2009).
- ¹⁶L. Khomenkova, F. Gourbilleau, J. Cardin, and R. Rizk, *Physica E* **41**, 1048 (2009).
- ¹⁷D. Navarro-Urrios, A. Pitanti, N. Daldosso, F. Gourbilleau, L. Khomenkova, R. Rizk, and L. Pavesi, *Physica E* **41**, 1029 (2009).
- ¹⁸M. J. A. de Dood, L. H. Slooff, A. Polman, A. Moroz, and A. van Blaaderen, *Phys. Rev. A* **64**, 033807 (2001).
- ¹⁹D. E. McCumber, *Phys. Rev.* **136**, A954 (1964).
- ²⁰W. J. Miniscalco, *J. Lightwave Technol.* **9**, 234 (1991).
- ²¹B. J. Ainslie, S. P. Craig-Ryan, S. T. Davey, J. R. Armitage, C. G. Atkins, J. F. Massicott, and R. Wyatt, *IEE Proc.-J: Optoelectron.* **137**, 205 (1990).
- ²²B. J. Ainslie, *J. Lightwave Technol.* **9**, 220 (1991).
- ²³P. Pellegrino, B. Garrido, J. Arbiol, C. Garcia, Y. Lebour, and J. R. Morante, *Appl. Phys. Lett.* **88**, 121915 (2006).
- ²⁴J. S. Chang, J.-H. Jhe, M.-S. Yang, J. H. Shin, K. J. Kim, and D. W. Moon, *Appl. Phys. Lett.* **89**, 181909 (2006).
- ²⁵F. Gourbilleau, M. Levalois, C. Dufour, J. Vicens, and A. Rizk, *J. Appl. Phys.* **95**, 3717 (2004).